an Article from

Journal of Robotics and Mechatronics

4F Toranomon Sangyo Bldg., 2-29, Toranomon 1-chome, Minatoku, Tokyo 105-0001, Japan
Tel. +813-3508-0051, Fax: +813-3592-0648, E-mail: TAE00762@niftyserve.or.jp

Paper:

Measurement of Human Hand Impedance in Dual Arm Configurations

Yusaku Takeda, Yoshiyuki Tanaka, and Toshio Tsuji

Department of Artificial Complex Systems Engineering
Graduate School of Engineering, Hiroshima University
1-4-1 Kagamiyama, Higashi-Hiroshima, Hiroshima 739-8527, Japan
E-mail: takeda@bsys.hiroshima-u.ac.jp

[Received August 6, 2004; accepted September 28, 2004]

Dynamic characteristics of a human extremity are usually expressed using the mechanical impedance. This paper examines hand impedance in dual arm movements while posture was maintained in dual-arm configurations. The results of experiments show that the orientation of viscosity ellipses roughly agrees with the human sagittal axis, tending to be oriented similar to stiffness ellipses. Viscosity and stiffness amplitude and orientation exceed those of single arm. Our results will be used in human-robot cooperation systems and in analyzing human movements.

Keywords: human movements, hand impedance characteristics, dual arm posture, joint impedance

1. Introduction

A human uses his or her both hands effectively to diverse tasks that cannot be implemented by a single hand. Let us consider, for example, the task of carrying heaped loads smoothly, in which we must hold dual arms supporting loads firmly while making the hand soft on the horizontal plane to maintain the balance. In the task of placing a load on a platform, a human may switch task strategies using a single arm or dual arms according to the contact between the load and platform. For complicated tasks requiring high precision, hand motion is stabilized by coordinating left and right arms to maximize efficiency. Hence humans change dual arm movements according to the task objective and the contact with the environment.

Hand impedance regulation represented by compliance/stiffness seen in upper arm motion is important to designing human skillful movements. Mussa-Ivaldi [1] estimated hand stiffness while maintaining posture of a single arm for the first time. They showed that hand stiffness depended strongly on upper arm posture and a human changed stiffness size, but its orientation. Dolan et al. [2] and Tsuji et al. [3, 4] estimated hand impedance including stiffness, viscosity, and inertia, and found that stiffness and viscosity were qualitatively similar characteristics. Tsuji et al. [5] clarified that hand viscoelasticity changed largely with regard to the muscle contraction levels, and showed that the joint viscoelasticity could be predicted from muscle contraction levels estimated from the myoelectric signals. On the other hand, Gomi et al. [6] measured hand impedance during the multi-joint movements and pointed out that hand stiffness during motion changed more than that while maintaining same posture. The above studies examinded hand impedance only for horizontal 2-joint motion in a single arm.

Dual arm motion is measured and analyzed versus studies on a single arm. Garvin et al. [7] simulated cooperative dual arm motion and showed that a straight-line trajectory planned with the minimum evaluation of jerk of the operated object and the hand agreed well with the hand trajectory actually measured. Desai et al. [8] used a dynamic model gripped by a pair of 2-joint arms for simulation, and showed that a straight-line trajectory planning based on a minimum evaluation of joint torque agreed well with the hand trajectory actually measured. However these simulation results may largely change depending on the joint compliance/stiffness of each arm. To better clarify dual arm motion in voluntary movements, we must know musculoskeletal impedance in dual arm multi-joint motion.

On the other hand, few studies have measured hand impedance in dual arm multi-joint movements. Kitamura et al. [9] state that a human regulates dual hand impedance based on compliance/stiffness of the operated object, but they do not show the relationship between posture and hand impedance. Li et al. [10] measured and analyzed the relationship between handle rotational stiffness of bicycle and dual hand force, showing that increasing inner force by the dual hand caused handle rotational stiffness to rise. They did not measure hand impedance itself and the dual hand impedance regulation by changes of the arm posture was not clarified.

In this paper, we conducted experiments in measuring hand impedance while maintaining dual arm posture, and clarify hand impedance according to the dual arm configuration. Section 2 explains experiments measuring dual hand impedance we implemented. Section 3 discusses dual hand impedance measured in the experiments while a maintained posture.

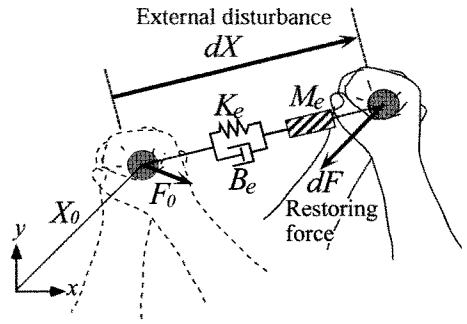

Fig. 1. Schematic description of hand impedance.

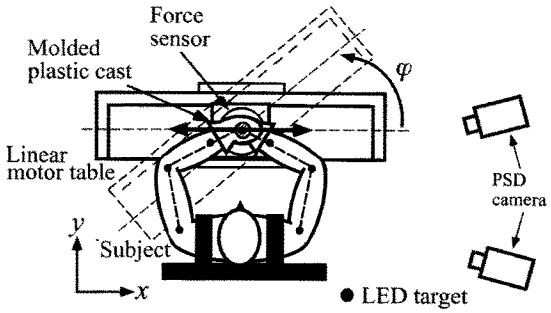

Fig. 2. Experimental apparatus.

2. Measurement of Hand Impedance Based on Dual Arm Configurations

2.1. Methods

Let us consider estimation of hand impedance based on dual arm configurations by the experiments. As shown in **Fig.1**, when an external disturbance is applied to a subject's hand, the dynamic properties of hand can be approximated with mechanical impedance model on a 2D plane as follows:

$$M_e\ddot{X}(t)+B_e\dot{X}(t)+K_e(X(t)-X_v(t))=F(t) \quad . \quad (1)$$

where $F(t)\in\Re^2$ is the force exerted by the hand to the environment, $X(t)\in\Re^2$ the hand position, $X_v(t)\in\Re^2$ the virtual trajectory of the hand. M_e, B_e, and $K_e\in\Re^{2\times2}$ are hand inertia, viscosity, and stiffness matrices. M_e is equivalent inertia representing upper extremities inertia in task space that changes based on arm mass and postures [11]. B_e and $K_e\in\Re^{2\times2}$ also depend on the viscoelastic properties of skeletal muscles, low-level neural reflexes and passive elements such as skins and vein. Assuming the onset time t_0 of external disturbance, dynamic hand properties at time t are given from Eq.(1):

$$M_e d\ddot{X}(t)+B_e d\dot{X}(t)+K_e dX(t)=dF(t) \quad . \quad . \quad . \quad (2)$$

here $dX(t)=X(t)-X(t_0)$, $dF(t)=F(t)-F(t_0)$.

This paper measures hand position x_{φ_i} and hand force F_{φ_i} in task coordinates on the 2D plane by changing relative angle φ_i between the subject and the orientation of motion (**Fig.2**). We use the following equation that represents Eq.(2) for one dimension with regards to motion direction φ_i to estimate M_{φ_i}, B_{φ_i}, and K_{φ_i} using the least squares method:

$$M_\varphi d\ddot{x}_{\varphi_i}(t)+B_{\varphi_i}d\dot{x}_{\varphi_i}(t)+K_{\varphi_i}dx_{\varphi_i}(t)=dF_{\varphi_i}(t) \quad (3)$$

where the hand inertia matrix is assumed to be symmetrical matrix and its element as follows:

$$M_e=\begin{bmatrix} M_{xx} & M_{xy} \\ M_{xy} & M_{yy} \end{bmatrix} \quad . \quad . \quad . \quad . \quad . \quad . \quad . \quad . \quad . \quad . \quad . \quad (4)$$

The relationship between M_{φ_i} and M_e that was obtained from Eq.(3) is as follows:

$$M_{\varphi_i}=\cos^2\varphi_i M_{xx}-2\sin\varphi_i\cos\varphi_i M_{xy}+\sin^2\varphi_i M_{yy}. \quad (5)$$

The following simultaneous equation is obtained by summarizing estimated hand inertia M_{φ_i} in each direction of motion φ_i $(i=1,2,\cdots,n:\ n\geq3)$:

$$\begin{bmatrix} M_{\varphi_1} \\ M_{\varphi_2} \\ \vdots \\ M_{\varphi_n} \end{bmatrix}=H\begin{bmatrix} M_{xx} \\ M_{xy} \\ M_{yy} \end{bmatrix} \quad . \quad . \quad . \quad . \quad . \quad . \quad . \quad . \quad . \quad . \quad (6)$$

where $H\in\Re^{n\times3}$ is a coefficient matrix which is assumed to be of full rank with respect to the column. M_e is found by multiplying both sides of Eq.(6) from the left by pseudo inverse matrix $H^{\#}$. B_e and K_e are found similarly.

2.2. Experimental Apparatus [12]

Figure 2 shows experimental apparatus, which uses a linear motor table (Nippon Thompson Co., LTD.) with one degree of freedom using a magnetic drive to forcibly displace the subject's hand. The table has a 6-axis force sensor (BL Autotec Co., LTD., resolution: translation force x-axis, y-axis: 0.05N, z-axis: 0.15N, torque: 0.003Nm) to measure force F the subject applies to the handle. Handle position X_t is measured by the encoder (resolution: 2μm). The rotary motor installed under the table controls table direction φ. Two PSD cameras (Hamamatsu Photonix Co., LTD.) measure the arm posture of a subject by detecting the LED targets attached to the subject's shoulder and elbow and table handle. Error is approximately 3% in absolute coordinates when 3D coordinates are restored from LED measurement.

This paper assumes that hand inertia, stiffness, and viscosity are constant during external disturbance for measurement. This depends strongly on the external disturbance pattern applied to the subject's hand. This external disturbance must end quickly with the possible smallest amplitude. Irregular signals must have sufficient bandwidth to obtain a highly precise estimation [3–5]. To satisfy these requirements, this paper used an external disturbance pattern that returned to the pre-displacement in 0.3s after displacement from initial position $X(t_0)$. **Fig.3** is an example of handle position and force displacement measured. External disturbance applied along toward the x-axis (**Fig.2**) and shows position dx_φ, velocity $d\dot{x}_\varphi$, acceleration $d\ddot{x}_\varphi$, and force sensor output dF_φ from the top.

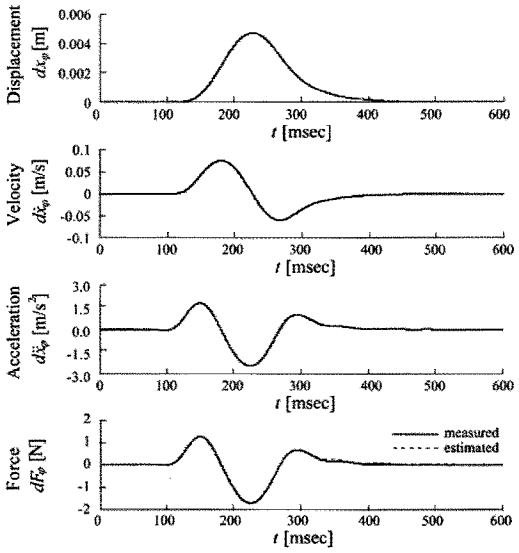

Fig. 3. Example of signals measured by table handle.

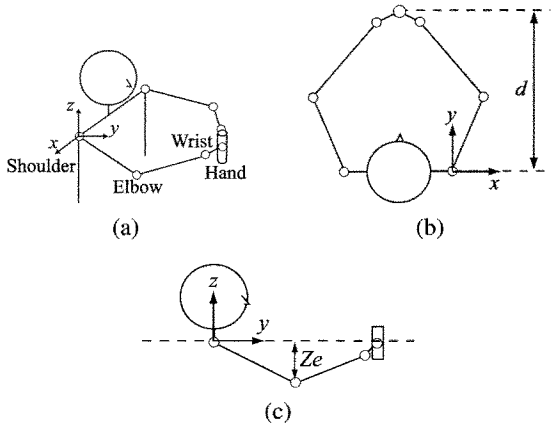

Fig. 4. Experimental conditions for arm posture.

Solid lines of force are measured and break lines are calculated using Eq.(3) from M_φ, B_φ, and K_φ. This enables us to obtain estimated results roughly equal to the true known physical quantity (stiffness, inertia) and estimating hand impedance precisely.

3. Hand Impedance Characteristics Based on Dual Arm Configuration

3.1. Experimental Method

As shown in **Fig.2**, a subject sits on a chair near toward the front of the table and subject's shoulder is fixed to it with a belt. The hand and the wrist were fixed by a plastic cast tightly attached to the table handle in order to eliminate the need for a voluntary grasping action which might influence the measurements of hand impedance. In the experiments, we changed the table direction to $\varphi = 0, \pi/4, \pi/2, 3\pi/4$ rad when the subject was requested

Table 1. Measured parameters K_{φ_i}, B_{φ_i}, M_{φ_i}, where the distance between the hand and subject changes. Mean and standard deviations for 5 estimated results are shown for three subjects.

Subject	Hand position d [m]	Table angle [deg]	Stiffness [N/m] K_{φ_i}	Viscosity [Ns/m] B_{φ_i}	Inertia [kg] M_{φ_i}
A	0.35	0	196.72±66.741	34.55±2.104	3.93±0.158
		45	309.96±33.623	35.56±1.869	3.13±0.146
		90	564.38±123.475	34.75±0.797	2.59±0.150
		135	386.41±34.289	35.31±0.809	2.99±0.090
	0.40	0	191.21±19.475	17.85±0.494	3.97±0.026
		45	536.25±35.492	38.00±0.769	3.59±0.032
		90	808.59±72.011	49.64±0.576	3.37±0.026
		135	504.91±40.011	36.93±0.935	3.31±0.116
	0.45	0	181.01±5.270	15.88±0.517	3.37±0.073
		45	539.70±54.295	43.74±0.925	3.77±0.035
		90	869.00±74.638	61.77±0.736	3.49±0.049
		135	583.87±52.560	42.92±1.816	3.57±0.126
B	0.35	0	242.37±25.532	21.26±0.462	4.03±0.031
		45	342.66±59.094	21.63±1.584	3.12±0.083
		90	487.79±65.718	29.37±1.325	2.89±0.099
		135	304.67±52.074	32.10±1.205	3.47±0.047
	0.40	0	201.89±25.161	18.81±2.504	3.92±0.031
		45	474.55±24.728	25.81±1.033	3.34±0.060
		90	728.50±66.575	34.80±1.515	3.23±0.068
		135	947.21±139.198	36.58±0.930	3.74±0.029
	0.45	0	238.82±25.437	16.91±0.656	3.85±0.031
		45	739.86±139.707	54.91±4.258	3.19±0.120
		90	1130.10±165.206	74.56±1.924	3.39±0.105
		135	586.23±91.454	43.61±0.642	3.50±0.067
C	0.35	0	174.21±29.596	31.98±2.328	4.35±0.055
		45	145.36±34.388	41.72±2.252	2.96±0.060
		90	262.42±39.531	54.46±5.397	2.04±0.109
		135	250.63±34.663	37.57±19.530	2.74±1.331
	0.40	0	104.04±21.010	26.13±0.548	3.87±0.034
		45	238.96±50.742	44.53±3.151	3.05±0.113
		90	396.26 ±94.152	58.23±37.987	1.83±1.304
		135	203.26±67.665	44.52±26.013	2.43±1.312
	0.45	0	115.27±13.694	23.95±0.665	3.82±0.047
		45	238.74±79.966	53.40±3.870	2.89±0.156
		90	446.17±99.798	71.84±14.386	1.20±0.397
		135	129.43±47.310	50.24±28.300	2.35±1.300

to maintain the posture and applied external disturbance on the subject's hand from eight directions. We then measured the hand position and time changes in hand force. As shown in **Fig.4(a)**, task coordinates has the x-axis to left and right of the body, the y-axis forward and backward, the z-axis for the upward and downward directions.

In this paper, we measured hand impedance of three subjects (male college students aged of 22 to 24 years) while they maintained the dual arm posture. We then had them do as follows and monitored changes in hand impedance caused by changing posture:

I. The upper arm is maintained on the horizontal plane containing the wrist, elbow, and shoulder joints and hand distance is changed to $d = 0.35, 0.40$ and 0.45m (**Fig.4(b)**).

II. The hand distance is maintained at $d = 0.40$m, and the distance of elbow joint from the horizontal plane containing the wrist and shoulder joints is changed to $Z_e = 0.0$ and 0.1m (**Fig.4(c)**).

The next section focuses on symmetrical components of the hand impedance matrix as done by Mussa-Ivaldi et al. and Tsuji et al. and analyzes changes in hand impedance caused by posture based on dual arm configurations using impedance ellipses.

3.2. Changes in Hand Impedance Caused by the Hand Position

Table 1 shows hand impedance in each direction of mo-

Table 2. Measured hand impedance parameters of dual arms for the three subjects, where the distance between the hand and subject changes.

Subject	Hand posture d [m]	Stiffness [N/m]		Viscosity [Ns/m]		Inertia [kg]	
		K_{xx}	K_{xy}	B_{xx}	B_{xy}	M_{xx}	M_{xy}
		K_{yx}	K_{yy}	B_{yx}	B_{yy}	M_{yx}	M_{yy}
A	0.35	180.54	−38.22	34.95	0.13	3.10	0.07
		−38.22	548.20	0.13	35.14	0.07	1.76
	0.40	201.56	15.67	19.71	0.53	3.13	0.14
		15.67	818.93	0.53	51.50	0.14	2.53
	0.45	170.21	36.30	15.98	4.71	2.84	0.32
		36.30	858.20	4.71	61.88	0.32	2.44
B	0.35	238.02	−13.71	22.03	−5.24	3.22	−0.18
		−13.71	483.43	−5.24	30.14	−0.18	2.08
	0.40	214.37	−15.61	21.01	−5.38	3.18	−0.20
		−15.61	740.99	−5.38	36.99	−0.20	2.49
	0.45	228.11	76.82	18.67	5.65	2.98	−0.16
		76.82	1119.39	5.65	76.32	−0.16	2.52
C	0.35	164.05	−52.63	30.2	2.07	3.44	0.11
		−52.63	252.26	2.07	52.7	0.11	1.14
	0.40	117.10	17.85	27.30	0.00	3.09	0.31
		17.85	298.98	0.00	59.40	0.31	1.05
	0.45	60.80	66.95	25.91	1.58	2.94	0.27
		66.95	391.70	1.58	73.80	0.27	1.12

Table 3. Geometrical parameters of measured hand impedance ellipses for dual arms, where the distance between the hand and the subject changes for three subjects.

Subject	Hand position d [m]	Stiffness ellipses		Viscosity ellipses		Inertia ellipses	
		Orientaion [deg]	Shape	Orientaion [deg]	Shape	Orientaion [deg]	Shape
A	0.35	95.87	3.13	64.05	1.01	2.99	1.77
	0.40	88.55	4.07	89.04	2.61	12.60	1.26
	0.45	86.99	5.11	84.21	4.02	29.04	1.33
B	0.35	93.19	2.04	116.12	1.68	8.56	1.58
	0.40	91.70	3.47	106.98	2.00	14.94	1.33
	0.45	85.11	5.08	84.46	4.24	17.14	1.22
C	0.35	115.02	1.98	84.77	1.76	2.77	3.04
	0.40	84.45	2.61	90.00	2.18	8.40	3.14
	0.45	78.98	8.47	88.11	2.86	8.34	2.75

tion measured in task assignment I. This table lists measured parameters M_{φ_i}, B_{φ_i}, and K_{φ_i} (mean and standard deviation) using measurement (60 trials) of five sets of task assignment I for subjects A to C. **Table 2** shows elements of the dual hand impedance matrix in each posture calculated using Eq.(6) from the mean values in **Table 1**. **Fig.5** shows the dual hand impedance ellipses calculated using measured results in **Table 2** for the distance, $d = 0.35, 0.45$m (See **Fig.4(b)**).

The major axis of the inertia ellipse inclines toward the x-axis of task coordinates. The major axis of the stiffness and viscosity ellipse inclines toward the y-axis of task coordinates regardless of the hand position. **Table 3** shows results for calculating the ratio of the major axis of each ellipse to the angle of the x-axis in task coordinates and the minor axis. This table indicates that the shape of the inertia ellipse tends to approach the true circle when the hand position leaves the body. It shows that the shape of the stiffness and viscosity ellipses has roughly the same inclination regardless of the hand position and that the shape lengthens as the hand position leaves the body and

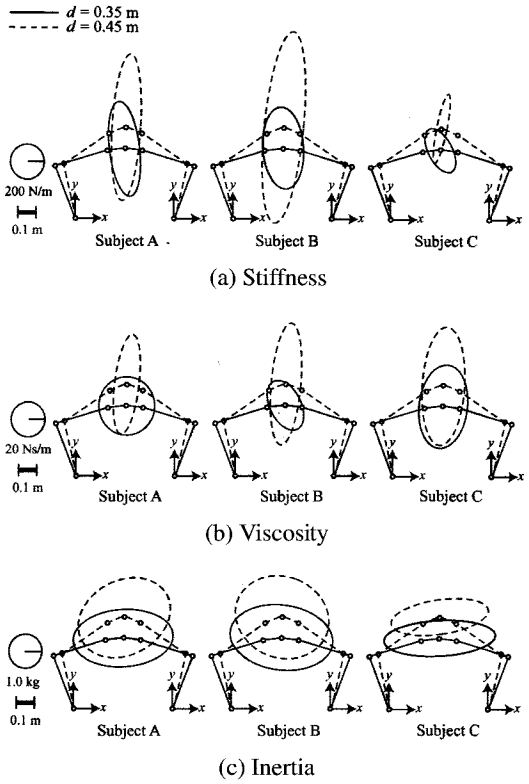

Fig. 5. Measured impedance ellipses for dual arms, where the distance between the hand and subject changes for three subjects.

is regulated in orientation of the y-axis in task coordinates, but not adjusted.

3.3. Changes in Hand Impedance Caused by Elbow Joint Position

Similarly to the task assignment I, **Tables 4** and **5** show dual hand impedance (40 trials) in each direction of motion and each element of the dual hand impedance matrix in each posture. **Fig.6** shows dual arm impedance ellipses for distance, $Z_e = 0.0, 0.1$m (See **Fig.4(c)**). From the figure, and each ellipse has the same trend in the orientation of major axis as the task assignment I regardless of the position of elbow joint. Similarly to the task assignment I, **Table 6** lists results for calculating geometrical features of each ellipse. From this table, the inclinations of the stiffness and viscosity ellipses are roughly the same regardless of the position of the elbow joint and the shape of the stiffness ellipse tends to lengthen as the position of the elbow joint drops from the horizontal plane, resulting in viscosity and inertia ellipses approaching a true circle. These results imply that hand stiffness is adjusted by dropping the elbow joint from the horizontal plane, but viscosity does not change as much as stiffness.

3.4. Discussion

From the measurement results, we found that stiffness and viscosity ellipses lengthen when the hand position left

Table 4. Measured parameters K_{φ_i}, B_{φ_i}, M_{φ_i}, where the distance between the plane and the subject's elbow changes. Mean and standard deviations for 5 results are shown for three subjects.

Subject	Elbow position Z_e [m]	Table angle [deg]	Stiffness [N/m] K_{φ_i}	Viscosity [Ns/m] B_{φ_i}	Inertia [kg] M_{φ_i}
A	0.00	0	166.96±17.355	22.69±0.534	3.72±0.022
		45	547.21±42.368	31.38±1.325	3.28±0.112
		90	900.81±50.787	49.26±1.769	2.89±0.036
		135	501.16±48.617	35.33±1.247	3.20±0.070
	0.10	0	167.71±19.811	20.14±0.338	3.54±0.042
		45	644.81±70.239	37.24±0.982	3.21±0.057
		90	1074.14±53.169	56.58±3.318	2.93±0.101
		135	694.30±72.271	43.66±2.614	3.24±0.161
B	0.00	0	121.61±57.409	23.23±0.722	3.66±0.080
		45	758.16±69.972	42.61±2.016	3.30±0.074
		90	1107.53±85.452	60.15±4.842	2.43±0.089
		135	609.74±63.797	44.91±0.884	3.00±0.063
	0.10	0	199.19±23.409	21.26±0.948	3.52±0.033
		45	844.33±71.909	35.20±0.954	2.73±0.081
		90	1278.39±83.418	52.13±3.290	2.60±0.053
		135	390.88±48.856	44.83±2.445	2.66±0.088
C	0.00	0	207.40±45.474	26.69±1.126	3.90±0.059
		45	413.56±35.957	48.76±1.394	3.00±0.037
		90	432.09±48.220	76.30±4.426	1.93±0.119
		135	323.36±31.459	54.95±7.702	2.63±0.592
	0.10	0	172.46±28.018	27.32±0.789	3.63±0.027
		45	474.34±105.498	48.83±3.577	2.94±0.056
		90	871.30±93.782	73.13±2.602	2.81±0.138
		135	380.07±52.665	51.21±2.975	2.77±0.087

Table 5. Measured hand impedance parameters of dual arms for three subjects where the distance between the plane and subject's elbow changes.

Subject	Elbow position Z_e [m]	Stiffness [N/m] K_{xx}	K_{xy}	Viscosity [Ns/m] B_{xx}	B_{xy}	Inertia [kg] M_{xx}	M_{xy}
		K_{yx}	K_{yy}	B_{yx}	B_{yy}	M_{yx}	M_{yy}
A	0.00	162.11	23.02	21.38	−1.98	2.96	0.04
		23.02	895.96	−1.98	47.95	0.04	2.12
	0.10	192.02	−24.75	21.18	−3.21	2.80	−0.01
		−24.75	1098.45	−3.21	57.63	−0.01	2.20
B	0.00	156.30	74.21	24.26	−1.15	2.98	0.15
		74.21	1142.22	−1.15	61.19	0.15	1.75
	0.10	138.60	226.73	22.92	−4.82	2.61	0.04
		226.73	1217.80	−4.82	53.79	0.04	1.69
C	0.00	216.38	75.86	23.74	3.17	3.02	0.39
		75.86	441.07	3.17	73.35	0.39	1.05
	0.10	162.85	47.14	30.84	−1.19	2.87	0.08
		47.14	710.80	−1.19	62.17	0.08	1.46

Table 6. Geometrical parameters of measured hand impedance ellipses for dual arms where the distance between the plane and the subject's elbow changes for three subjects.

Subject	Elbow position Z_e [m]	Stiffness ellipses Orientaion [deg]	Shape	Viscosity ellipses Orientaion [deg]	Shape	Inertia ellipses Orientaion [deg]	Shape
A	0.00	88.20	5.56	94.23	2.27	2.77	1.39
	0.10	91.56	5.74	94.99	2.77	−1.40	1.28
B	0.00	85.72	7.61	91.79	2.53	6.78	1.73
	0.10	78.60	13.60	98.67	2.46	2.26	1.55
C	0.00	72.99	2.40	86.36	3.12	10.73	3.16
	0.10	85.12	4.50	92.17	2.02	3.45	1.97

for the body in the task assignment I and that the stiffness ellipse tends to lengthen when the elbow joint dropped below the horizontal plane in the task assignment II and the viscosity ellipse approaches a true circle. As seen in the stiffness ellipse of subject C in the task assignment I and

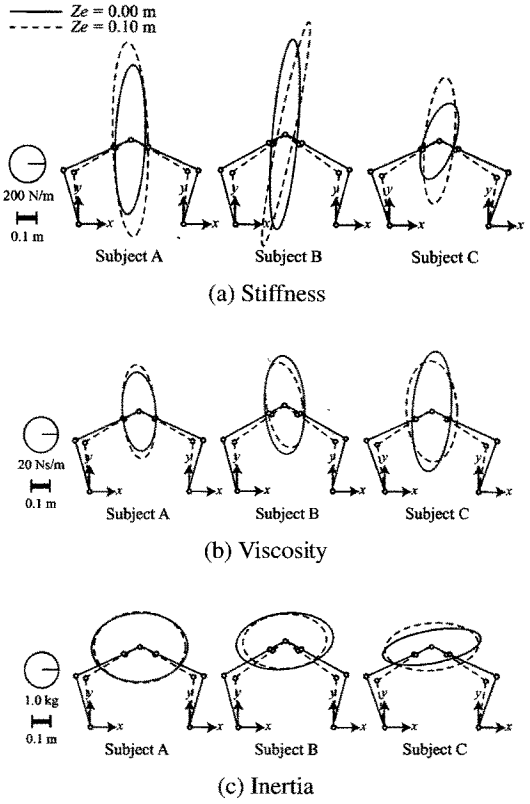

Fig. 6. Measured impedance ellipses for dual arms where the distance between the plane and the subject's elbow changes for three subjects.

Table 7. Measured hand impedance parameters of single and dual arm at hand position $d = 0.45$m.

	Stiffness [N/m] K_{xx}	K_{xy}	Viscosity [Ns/m] B_{xx}	B_{xy}	Inertia [kg] M_{xx}	M_{xy}
	K_{xy}	K_{yy}	B_{xy}	B_{yy}	M_{xy}	M_{yy}
Right arm	184.75	−143.65	7.52	−7.45	1.51	−0.88
	−143.65	317.84	−7.45	14.00	−0.88	1.43
Left arm	201.75	177.30	9.51	7.49	1.61	0.74
	177.30	284.45	7.49	14.85	0.74	1.07
Dual arm	406.95	115.74	18.42	1.94	3.25	−0.19
	115.74	1180.12	1.94	47.65	−0.19	2.46

the viscosity ellipse of subject A in the task assignment II, these cases differed from other subjects. These differences are caused by the human multi-joint link mechanism, and an extra torque generated in joints compared with other subjects at the time of measuring the hand impedance. We considered the differences between left and right hand impedance measured of a single arm, in the task assignment I in the same posture as when measuring dual hand impedance and considered those differences.

Table 7 shows the measured hand impedance matrix for the left, right, and dual arms at hand position $d = 0.45$m in the task assignment I. **Figs.7** and **8** show hand impedance ellipses for the left, right, and dual arms to-

Table 8. Comparison of geometrical parameters of measured hand impedance ellipses of single and dual arms at hand position $d = 0.45$m.

	Stiffness ellipses			Viscosity ellipses			Inertia ellipses		
	Area $[\times 10^6(\text{N/m})^2]$	Orientaion [deg]	Shape	Area $[\times 10^2(\text{Ns/m})^2]$	Orientaion [deg]	Shape	Area $[(\text{kg})^2]$	Orientaion [deg]	Shape
Right arm	0.12	122.57	4.41	1.56	123.25	7.16	4.35	136.30	3.99
Left arm	0.08	51.56	6.97	2.67	54.81	4.76	3.69	34.98	3.85
Summated impedances of right and left arm	0.73	81.34	1.59	15.44	89.81	1.69	24.44	12.15	1.28
Measured impedance of dual arm	1.47	81.67	3.07	27.46	86.22	2.61	25.00	12.84	1.36

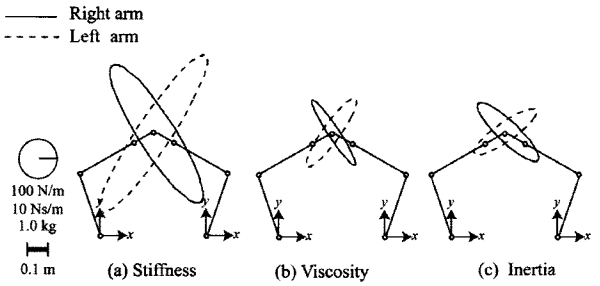

Fig. 7. Measured impedance ellipses for single arms at hand position $d = 0.45$m.

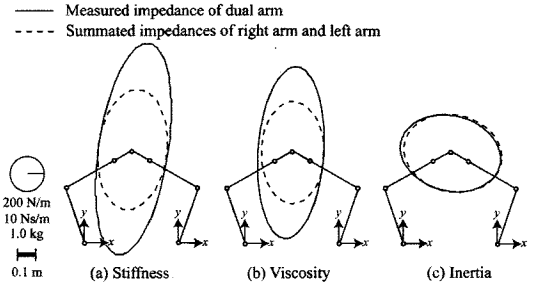

Fig. 8. Measured and computed impedance ellipses for dual arms at hand position $d = 0.45$m.

gether with postures. Solid lines of each ellipse in **Fig.8** show the dual arm impedance ellipse, while break lines and a summated ellipse for each impedance of the left and right arms. Geometrical features are summated to **Table 8** the same as in the task assignments I and II to show results of calculating areas of ellipses.

Figure 7 shows that the major axis of stiffness and viscosity ellipses closes to a line between the subject's hand and shoulder, consistent with conventional studies [1–3]. Hand impedance of the left arm is roughly symmetrical to that of the right arm (**Table 8**).

The area and orientation of viscoelasticity ellipses of dual arms and of single arms (**Table 8**) differ greatly compared to results to the single arm (**Fig.7**). As ellipses shown by solid and break lines are compared, inertia is roughly the same. Measured stiffness and viscous ellipses have roughly the same orientation in comparing their major axes, but major axes of the summated ellipses of left and right arm stiffness and viscosity are nearly twice as long as major ones of ellipses of the measured dual arm.

Desai et al. [8] show in experiments that inner force acting on dual arms increases with increasing hand velocity when subjects move dual arms in straight-lines. They simulated a model representing dual arms with a pair of 2-joint arms and planned a straight-line trajectory and showed that the trajectory, especially along the y-axis of task coordinates, did not match that measured in the experiment, possibly due to only the sum of hand stiffness and viscosity of a single arm representing the orientation of hand impedance of dual arms, but could not represent size in the y-axis orientation of the task coordinates. Inner force changes between left and right hands generated by perturbation acting on the hand when hand impedance of dual arms is measured, which may affect measurement of hand stiffness and viscosity in the y-axis orientation of task coordinates.

Changes in measurement of hand impedance taking into account the inner force acting between dual hands, those in muscular activity, and how hand stiffness and viscosity of dual arms relate remain to be clarified.

4. Conclusions

This paper investigated hand impedance based on dual arm configuration during upper arm posture changes. The major results are as follows:

(1) Hand stiffness, viscosity, and inertia of dual hands differ more than those of a single arm.

(2) The major axis of the dual hand viscosity ellipse directed toward the y-axis of task coordinates and its orientation resemble that for hand stiffness.

(3) The major axis of the dual hand inertia ellipse directed toward the x-axis of task coordinates.

Measurement results were considerably dispersed in results measured for hand impedance.

Future research will improve measurement precision and clarify dual hand impedance in different postures with changes in viscoelasticity according to muscle contraction levels and hand force. We will analyze how hand impedance in dual arm configuration changes based on the environment. If hand impedance regulation depends

on dual arm configuration, it will be applicable to the development of dual-arm robots and welfare equipments taking into account the motion characteristics of the human arms.

Acknowledgements

This research was supported by Grant-in-Aid for Scientific Research of Japan Society for the Promotion of Science (15008210) and The Ministry of Education, Culture, Sports, Science and Technology (14750188 and 15360226), for which as are most grateful.

References:

[1] F. A. Mussa-Ivaldi, N. Hogan, and E. Bizzi, "Neural, mechanical and geometric factors subserving arm in humans," Journal of Neuroscience, Vol.5, No.10, pp. 2732-2743, 1985.

[2] J. M. Dolan, M. B. Friendman, and M. L. Nagarka, "Dynamics and loaded impedance components in the maintenance of human arm posture," IEEE Transaction on Systems, Man and Cybernetics, Vol.23, No.3, pp. 698-709, 1993.

[3] T. Tsuji, K. Goto, K. Ito, and M. Nagamachi, "Estimation of human hand impedance during maintenance of posture," Transactions of the Society of Instrument and Control Engineers, Vol.30, No.3, pp. 319-328, 1994 (in Japanese).

[4] T. Tsuji, P. Morasso, K. Goto, and K. Ito, "Human hand impedance characteristics during maintained posture in multi-joint arm movements," Biological Cybernetics, Vol.72, pp. 475-485, 1995.

[5] T. Tsuji, M. Moritani, M. Kaneko, and K. Ito, "An analysis of human hand impedance characteristics during isometric muscle contractions," Transactions of the Society of Instrument and Control Engineers, Vol.32, No.2, pp. 271-280, 1996 (in Japanese).

[6] H. Gomi, and M. Kawato, "Mechanical impedance of human arm during multi-joint movement in horizontal Plane," Transactions of the Society of Instrument and Control Engineers, Vol.32, No.3, pp. 369-378, 1996 (in Japanese).

[7] G. J. Garvin, M. Zefran, E. A. Henis, and V. Kumar, "Two-arm trajectory planning in a manipulation task," Biological Cybernetics, Vol.76, pp. 53-62, 1997.

[8] J. P. Desai, M. Zefran, and V. Kumar, "Two arm manipulation tasks with friction assisted grasping," Advanced Robotics, Vol.12, No.5, pp. 485-508, 1998.

[9] T. Kitamura, M. Katayama, X.-Z. Zheng, and K. Ito, "Identification of human hand impedance during cooperative manipulation with both hands," Proceedings of the 11th Symposium on Biological and Physiological Engineering, pp. 353-356, 1996 (in Japanese).

[10] Z. Li, K. Kubo, and S. Kawamura, "Effect of hand force on rotational stiffness of bicycle handle," Transactions of the Society of Instrument and Control Engineers, Vol.38, No.11, pp. 915-921, 2002 (in Japanese).

[11] N. Hogan, "The Machanics of Multi-joint Posture and Movement Control," Biological Cybernetics, Vol.53, pp. 1-17, 1985.

[12] T. Tsuji, Y. Kanji, T. Kato, M. Kaneko, and S. Kawamura, "Impedance training: can we regulate our hand impedance through training?" Transactions of the Society of Instrument and Control Engineers, Vol.35, No.10, pp. 1300-1306, 1999 (in Japanese).

[13] T. Tsuji, "Measuring viscoelasticity in human arm movements," Journal of the Society of Instrument and Control Engineers, Vol.35, No.9, pp. 689-695, 1996 (in Japanese).

[14] T. Flash, and I. Gurevich, "Model of motor adaptation and impedance control in human arm movements," Self-Organization, Computational Maps, and Motor Control, pp. 423-481, 1997.

[15] T. Yoshikawa, "Foundations of robot control," Corona Publishing CO.,LTD., pp. 109-131, 1988 (in Japanese).

Name:
Yusaku Takeda

Affiliation:
Department of Artificial Complex Systems Engineering, Hiroshima University

Address:
1-4-1 Kagamiyama, Higashi-Hiroshima, Hiroshima 739-8527, Japan

Brief Biographical History:
1996- Faculty of Engineering, Hiroshima University
2000- Graduate School of Engineering, Hiroshima University
2003- Japan Society for the Promotion of Science Fellows (DC2)

Main Works:
• Y. Takeda, T. Tsuta, and T. Iwamoto, "Multibody Dynamics Approach of Humerus-shoulder Complex, Driven by Muscloskeletal System and Application to the Elderly Stand-up Motion," Biomechanism, Vol.16, pp. 253-266, 2002.

Membership in Learned Societies:
• The Japan Society of Mechanical Engineers (JSME)
• Society of Biomechanisms (SOBIM) Japan

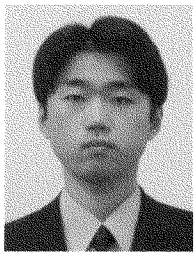

Name:
Yoshiyuki Tanaka

Affiliation:
Research associate, Department of Artificial Complex Systems Engineering, Hiroshima University

Address:
1-4-1 Kagamiyama, Higashi-Hiroshima, Hiroshima 739-8527, Japan

Brief Biographical History:
2001- Research Associate at Hiroshima City University
2002- Research Associate at Hiroshima University

Main Works:
• Y. Tanaka, N. Yamada, T. Tsuji, and I. Masamori, "Manipulability Analysis with Human Joint-Torque Characteristics of the Lower Extremity," Journal of the Society of Instrument and Control Engineers, Vol.40, No.6, pp. 612-618, 2004.

Membership in Learned Societies:
• The Robotics Society of Japan (RSJ)
• The Japanese Society of Instrumentation and Control Engineers (SICE)
• The Institute of Electrical Engineers of Japan (IEEJ)

Name:
Toshio Tsuji

Affiliation:
Department of Artificial Complex Systems Engineering, Hiroshima University

Address:
1-4-1 Kagamiyama, Higashi-Hiroshima, Hiroshima 739-8527, Japan

Brief Biographical History:
1985- Research Associate at Hiroshima University
1995- Associate Professor at Hiroshima University
2002- Full Professor at Hiroshima University

Main Works:
• T. Tsuji, P. Morasso, K. Goto, and K. Ito, "Human Hand Impedance Characteristics during Maintained Posture in Multi-Joint Arm Movements," Biological Cybernetics, Vol.72, pp. 475-485, 1995.

Membership in Learned Societies:
• Institute of Electrical and Electronics Engineers (IEEE)
• The Robotics Society of Japan (RSJ)
• The Japanese Society of Instrumentation and Control Engineers (SICE)
• The Institute of Electrical Engineers of Japan (IEEJ)